^{1}H NMR Studies of the Imidazole Complex of Cytochrome *c*: Resonance Assignment and Structural Characterization of the Heme Cavity

Weiping Shao, Hongzhe Sun, Yiming Yao, and Wenxia Tang*

State Key Laboratory of Coordination Chemistry, Nanjing University, Nanjing 210093, China

Received December 17, 1993[⊗]

Two-dimensional ^{1}H nuclear magnetic resonance exchange correlated spectroscopy (2D EXSY), 1D saturation transfer, and nuclear Overhauser effect (NOE) experiments have been utilized in conjunction with isotope labeling to allow a comprehensive assignment of the hyperfine shifted resonances in the low spin imidazole complex of cytochrome *c* (Im−cyt *c*). Various two-dimensional phase-sensitive experiments (EXSY, DQF-COSY, TOCSY) are combined to assign the majority of the heme pocket side-chain proton signals. 1D NOE and 2D NOESY spectra of Im−cyt *c* are presented. Qualitative interpretation of NOE data indicates the structure in the heme pocket of Im−cyt *c* has changed relative to cyt *c*. Large conformational changes are apparent on the methionine side of the heme in the environment of the axial ligand. On the basis of the NOEs observed, the nearly parallel orientation of the bound imidazole to the plane of His18 imidazole has also been obtained, which agrees with the characteristic EPR *g* values similar to that of cytochrome b_5.

Introduction

Cytochrome *c* (Cyt *c*), which transfers electrons along the respiratory chain from cyt *c* reductase to cyt *c* oxidase, is one of the most studied member of the important electron transfer proteins. X-ray structural analysis shows that in the native molecule, the low-spin Fe(III) lies in the plane of the porphyrin ring with fifth coordination site occupied by a nitrogen atom of the imidazole of histidine 18 and the remaining coordination site by the sulfur atom of methionine 80.[1,2] NMR studies, including analyses of paramagnetic pseudocontact shifts suggest that in the solution state the overall protein fold and the positions of most residues packed against the heme are similar to the molecular structure determined by X-ray crystallography.[3-5] Spectroscopic studies indicate that at neutral pH, the iron−sulfur (Met80) bond is weak in the oxidized state, being readily displaced by external ligands (such as imidazole et al.).[6-7] The protein undergoes a groove opening reaction allowing external ligand complexes of cyt *c* to form. To understand fully the cause of functional changes brought about by axial ligand substitution, CN^-, Py and N_3^- derivatives have been studied using ^{1}H and ^{13}C NMR methods, but the results were mainly limited in the assignments of some ^{1}H and ^{13}C resonances of heme methyl groups;[8-10] in no case could the data bear on the structural changes of cyt *c* induced by the breakage of the Fe−S bond due to an exogenous ligand displacing Met80.

This paper presents a series of one- and two-dimensional ^{1}H NMR studies aimed at characterizing the heme and ligand environment of the low spin imidazole complex of cytochrome *c* (Im−cyt *c*). The majority of the heme pocket side-chain proton signals have been identified. Changes in NOE patterns between the heme and certain residues, and several residues around the axial ligand are interpreted in terms of changes in the pocket structure. Some detail of the difference between Im−cyt *c* and cyt *c* is offered, and the orientation of the bound Im to porphyrin and His18 imidazole has also been determined.

Experimental Section

Preparation of Samples. Horse heart cyt *c* (VI) was obtained from Sigma Chemical Co. and purified as previously described.[11] Cyt *c* was dissolved in ^2H_2O, incubated at 60 °C for 2 h in order to exchange all the labile protons, and then lyophilized. NMR samples were prepared by dissolving weighed amounts of lyophilized cyt *c* in 1.0 M imidazole (Im) or deuterated imidazole ([$^2H_4$]Im) ^2H_2O solution, the final concentration of imidazole binding to cyt *c* (Im−cyt *c* or [$^2H_4$]Im−cyt *c*) for 1D NMR experiments was 5 mM, and 8 mM [$^2H_4$]Im−cyt *c* solution was used for 2D NMR experiments. The mixture of cyt *c* and [$^2H_4$]Im−cyt *c* in 1:1 molar ratio was prepared by dissolution of the lyophilate in ^2H_2O containing 0.04 M [$^2H_4$]Im, the concentration of cyt *c* was 8 mM. All samples were adjusted to pH 7.0 by adding small aliquots of ^{2}HCl and NaO^{2}H. The pH readings were uncorrected for the isotope effect.

^{1}H NMR Measurement. All ^{1}H NMR spectra were recorded at 319 K on Bruker AM-500 spectrometer equipped with an Aspect 3000 computer system. Typically, 16K data points over 33 kHz or 7.5 kHz band width for 1D ^{1}H spectra and 512 × 2048 time-domain data size with a sweep width of 33 kHz or 7.5 kHz in the ω_2 dimension for 2D ^{1}H spectra were used. The carrier was centered on the residual water peak which was suppressed by presaturation. Chemical-shift values for all the resonances are referenced to internal 1,4-dioxane at 3.743 ppm.

Saturation-Transfer Experiments. The ligation of Im can be represented by reaction (1). Signals belonging to the same nuclear

$$\text{cyt } c + \text{Im} \underset{k_{-1}}{\overset{k_1}{\rightleftharpoons}} \text{Im−cyt } c \qquad (1)$$

species which interconverts between two different chemical environments on a time scale comparable with the intrinsic relaxation times

[⊗] Abstract published in *Advance ACS Abstracts,* December 15, 1994.

(1) Takano, T.; Dickerson, R. E. *J. Mol. Biol.* **1981**, *153*, 79.
(2) Bushnell, G. W.; Louie, G. V.; Brayer, G. D. *J. Mol. Biol.* **1990**, *214*, 585.
(3) Feng. Y.; Roder, H.; Englander, S. W. *Biochemistry* **1990**, *29*, 3494.
(4) Feng, Y.; Roder, H.; Englander, S. W.; Wand, A. J.; Di Stefano, D. L. *Biochemistry* **1989**, *28*, 195.
(5) Feng, Y.; Wand, A. J.; Roder, H.; Englander, S. W. *Biophys. J.* **1991**, *59*, 323.
(6) Sutin, N.; Yandell, J. K. *J. Biol. Chem.* **1972**, *247*, 6932.
(7) Bechtold, R.; Gardinner, M. B.; Kazmi, A.; Van Hemelryck, B.; Isied, S. S. *J. Phys. Chem.* **1986**, *90*, 3800.
(8) Smith, M.; Mclendon, G. *J. Am. Chem. Soc.* **1981**, *103*, 1912.
(9) Yamamoto, Y.; Nanai, N.; Inoue, Y.; Chûjô, R. *Biochem. Biophys. Res. Commun.* **1988**, *151*, 262.
(10) Shao, W. P.; Yao, Y. M.; Liu, G. H.; Tang W. X. *Inorg. Chem.* **1993**, *32*, 6112.
(11) Brautigan, D. L.; Ferguson-Miller, S.; Margoliash, E. *Methods Enzymol.* **1978**, *53D*, 131.

0020-1669/95/1334-0680$09.00/0

can lead through magnetization transfer experiments to establish connectivities between resonances and to extend known assignments in one chemical environment to the other environment in equlibrium with the former.[12] For a sample containing both cyt c (designated a) and Im−cyt c (designated b), when $\tau_b \leq 10T_1^b$, where τ_b and T_1^b are the exchange time and the intrinsic spin−lattice relaxation time of Im−cyt c respectively, upon saturation of a signal in cyt c, a decrease in intensity of the same signal in Im−cyt c is obtained, which can be used to assign the resonances of Im−cyt c in conjunction with the recent assignments of cyt c resonances.[4,13,14] The overall experiment was performed by applying a 0.5 s presaturation decoupler pulse either on-resonance saturation transfer spectrum or off-resonance reference spectrum. On- and off-resonance frequencies were alternated every 16 scans. The difference spectra were generated by substracting the reference spectra from the decoupler on-resonance spectra, in which the phenomenon of saturation transfer was most evident.

NOE Experiments. Nuclear Overhauser enhancement (NOE) experiments can provide data on internuclear distances which are directly correlated with the molecular conformation. The NOE intensity can be related to the distance r between preirradiated and observed spin by an equation of the general form (2).[15−17]

$$\mathrm{NOE} \propto \frac{1}{\langle r^6 \rangle} f(\tau_c) \qquad (2)$$

In paramagnetic systems, NOEs are relatively difficult to observe because of the large intrinsic longitudinal relaxation rates. However, the paramagnetism quenches spin diffusion allowing the selective detection of primary NOEs in large proteins.[16,17] The resulting NOEs therefore reflect primarily an internuclear distance of <3 Å for nearest neighbor nuclei on the heme and <5 Å for the protons on the pocket residues.[15] For 1D NOE experiments, NOE difference spectra were obtained in a similar fashion as described for the saturation transfer experiment, 7200−9600 scans were collected per spectrum.

T_1 Measurements. T_1 values of the resonances in Im−cyt c were measured by using the inversion−recovery method. For the case of dominant electron−nuclear dipolar relaxation, the relaxation times can be used to estimate the distance of protons to the iron by using

$$\frac{T_1^i}{T_1^j} = \left(\frac{r_i}{r_j}\right)^6 \qquad (3)$$

where $r_{i(j)}$ is the distance from proton $i(j)$ to the paramagnetic center and $T_1 i(j)$ is the longitudinal relaxation time from spin $i(j)$. Thus, r_i for a spin can be determined by using $r_j = 6.1$ Å, T_1^j for the slowest relaxing heme methyl, and T_1^i for spin i.[18]

2D NMR Experiments. 2D experiments including EXSY, DQF-COSY, TOCSY, and NOESY spectra were carried out using standard methods and phase cycling procedures. The 2D EXSY spectra were acquired by using the same pulse sequence as NOESY experiment with 128 scans per t_1 value. Mixing times of 25 and 50 ms for the former and 150 ms for the latter were used. 2D TOCSY spectra were collected by using an MLEV-17 spin lock, with 64 scans per t_1 value. Mixing times of 29, 50, and 87 ms were chosen. Prior to Fourier transformation the 2D data matrix was multiplied after zero filling of the t_1 time domain by a phase-shifted sine bell window function in both t_1 and t_2.

Results and Discussion

I. Resonance Assignments of Im−cyt c. 1. Assignments of Hyperfine-Shifted Resonances. In order to observe cross-peaks due only to chemical exchange effects and to minimize NOEs, high temperature (319 K) and a short mixing time (25 or 50 ms) were used to record 2D EXSY spectra in which essentially all the prominent cross-peaks are attributted to chemical exchange.[5] From the ^{1}H NMR spectra of cyt c, a mixture of cyt c and Im−cyt c, and Im−cyt c, several resonances of cyt c and Im−cyt c in the downfield and upfield regions are well resolved due to the large scalar interaction.

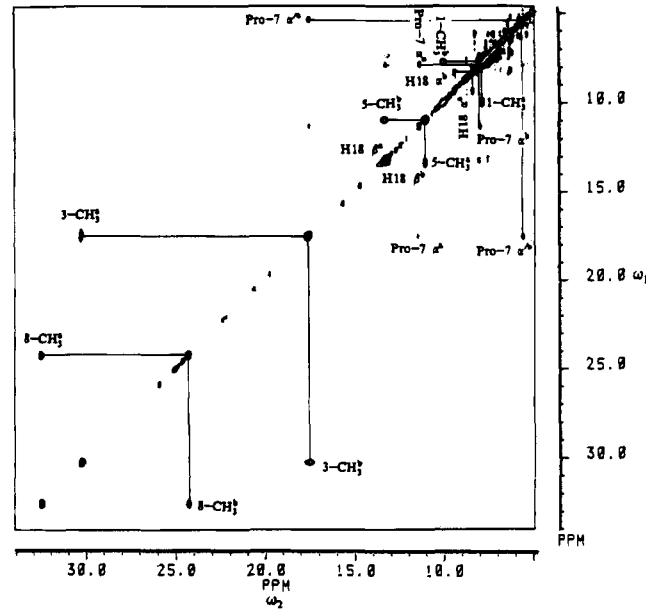

Figure 1. Downfield region of the 2D EXSY spectrum of a sample containing comparable amounts of cyt c and [^{2}H$_4$]Im−cyt c ($C_{\text{cyt c}}$ = 8 mM, $C_{[^2H_4]Im}$ = 0.04 M) at 319 K and pH 7.0 with mixing time 25 ms. Chemical shifts of resonances for cyt c and [^{2}H$_4$]Im−cyt c are read in the ω_2 dimension. *a* indicates cyt c; *b* indicates [^{2}H$_4$]Im−cyt c.

Heme Methyl Groups. In Figure 1, the 2D EXSY NMR spectrum of partially Im−cyt c (≈50%) is shown. Four signals (now at 24.20, 16.69, 14.05, and 10.69 ppm) show correlation with signals at 32.62, 30.26, 10.97, and 7.71 ppm, respectively. The chemical shifts of the latter four signals suggest that they belong to heme 8, 3, 5, and 1 methyl groups of cyt c,[13,14] so the observation of the above cross-peaks unequivocally identifies signals at 24.20, 16.69, 14.05, and 10.69 ppm as the 8, 3, 5 and 1-CH$_3$ resonances of the heme ring for Im−cyt c. The smaller chemical-shift range found for the heme methyl group resonances (the most shifted resonance appears at 24.20 ppm and the chemical-shift span of the methyl group resonances is about 14 ppm) than that for cyt c is indicative of a higher symmetry for the electron-spin distribution relative to cyt c.

Propionic-7. Propionic-7 (Pro-7) α, α′Hs in native cyt c have been assigned at 17.41 and 11.33 ppm.[14] In Figure 1, Pro-7 αH of cyt c, which overlaps with 3-CH$_3$ of Im−cyt c, shows not only the expected NOE at its geminal proton αH but also connectivities at 30.26 and 5.36 ppm. The former arises from 3-CH$_3$ of cyt c, so the latter is assigned to the Pro-7 αH of Im−cyt c. Similarly, Pro-7 α′H of cyt c gives corresponding signal at 7.80 ppm which can be assigned to Pro-7 αH of Im−cyt c.

His18. In the 2D EXSY spectrum (Figure 1), two resonances at 9.35 and 13.06 ppm of Im−cyt c correspond to the signals at 8.35 and 13.42 ppm of cyt c, respectively. These findings along with the previous assignments[4] identify signals at 9.35 and 13.06 ppm as αH and one of the βH of His18 in Im−cyt c.

Bound Imidazole. To focus on the environment and the orientation of the coordinated imidazole in the heme cavity, it

(12) Gupta, R. K.; Redfield, A. G. *Biochem. Biophys. Res. Commun.* **1970**, *41*, 273.
(13) Santos, H.; Turner, D. L. *FEBS Lett.* **1986**, *194*, 73.
(14) Satterlee, J. D.; Moensch, S. *Biophys. J.* **1987**, *52*, 101.
(15) Mclachlan, S. J.; La Mar, G. N.; Sletten, E. *J. Am. Chem. Soc.* **1986**, *108*, 1285.
(16) Thanabal, V.; de Ropp, J. S.; La Mar, G. N. *J. Am. Chem. Soc.* **1987**, *109*, 265.
(17) Dugad, L. B.; La Mar, G. N.; Unger, S. W. *J. Am. Chem. Soc.* **1990**, *112*, 1386.
(18) Peyton, D. H.; La Mar, G. N.; Pande, U.; Ascoli, F.; Smith, K. M.; Pandey, R. K.; Parish, D. W.; Bolognesi, M.; Brunori, M. *Biochemistry* **1989**, *28*, 4880.

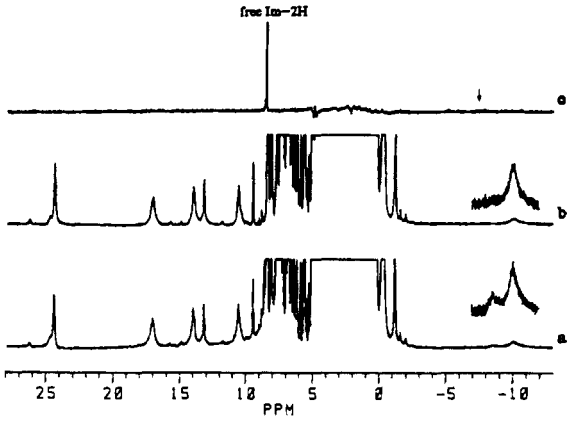

Figure 2. ^{1}H NMR spectra at 319 K and pH 7.0. Parts a and b show freshly prepared samples of Im−cyt *c* and [$^2H_4$]Im−cyt *c* ($C_{cyt\ c}$ = 5 mM, $C_{Im/[^2H_4]Im}$ = 1.0 M), respectively. Part c shows the saturation transfer difference spectrum with saturation of the 2H of the coordinated Im in Im−cyt *c*. The downward arrow indicates the peak being saturated.

Table 1. ^{1}H NMR Spectral Parameters[a] for Hyperfine-Shifted Heme Resonances of Im−cyt *c*

peaks	chem shifts (ppm)	T_1 (ms)
Heme 8-CH_3	24.20	112
3-CH_3	16.69	80
5-CH_3	14.05	126
1-CH_3	10.69	123
7−αH	5.36	
7−α′H	7.80	
His18 αH	9.35	136
βH	13.06	63
2H	−10.20	≈2
coord Imidazole 2H	8.70	≈2

[a] Chemical shifts with respect to dioxane at 3.743 ppm, determined at pH 7.0, 319 K.

is necessary to assign the signal of the bound imidazole in Im−cyt *c*. Figure 2a is the spectrum of freshly prepared Im−cyt *c*. Two broad peaks at −8.70 and −10.20 ppm appear in the upfield region. The large line width (≈400 Hz) and characteristic hyperfine shifts comparing with the resonances of the bound imidazole in both cyt b_5[19] and model complexes[20] suggest they arise from 2H of the axial imidazoles (His18 and the bound imidazole). The short T_1 values (≈2 ms) indicate they are located very close to the paramagnetic center (≈3.5 Å) and experience severe relaxation from delocalized spin density. In Figure 2b, the spectrum of [$^2H_4$]Im−cyt *c*, the disappearance of the resonance at −8.70 ppm shows that this peak arises from 2H of the bound Im, therefore, the other may be assigned to 2H of His18 ring. When preirradiating the resonance at −8.70 ppm, the chemical shift of 2H of the bound imidazole in the sample of Im−cyt *c*, the saturation is transferred to the 2H of the free imidazole, which confirms the above assignment (Figure 2c).

The chemical shifts and relaxation times of hyperfine shifted resonances of Im−cyt *c* are listed in Table 1.

2. Assignments of Some Resonances of Methyl-Containing Amino Acid Residues. The well-resolved porphyrin and axial ligand resonances in the mixture of cyt *c* and Im−cyt *c* can be easily assigned using only the 1D saturation transfer or 2D EXSY experimets. But, for the protein resonances, several experiments are performed.

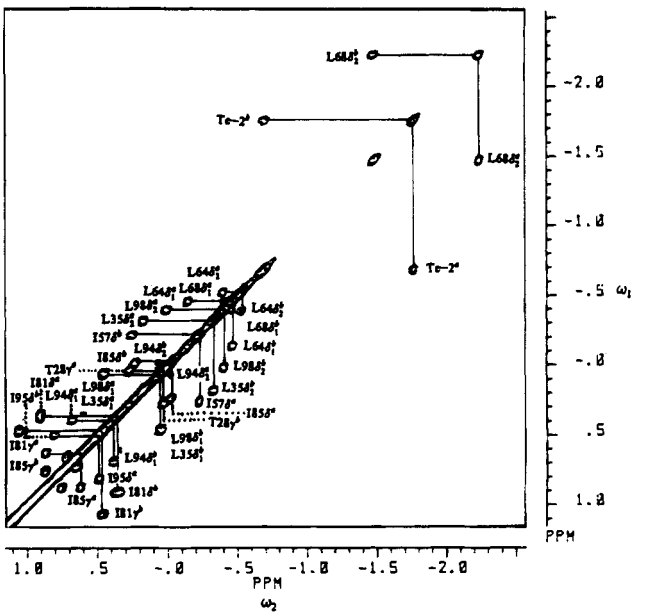

Figure 3. Aliphatic region of 2D EXSY spectrum of a samples containing comparable amounts of cyt *c* and [$^2H_4$]Im−cyt *c* ($C_{cyt\ c}$ = 8 mM, $C_{[^2H_4]Im}$ = 0.04 M) at 319 K and pH 7.0 with mixing time 50 ms. Chemical shifts of resonances for cyt *c* and [$^2H_4$]Im−cyt *c* are read in the ω_2 dimension. *a* indicates cyt *c*; *b* indicates [$^2H_4$]Im−cyt *c*.

The assignment strategy consisted of two steps. The first phase is the assignment of some resonances of Im−cyt *c* based on the previous assignments of native protein[4] using 2D EXSY. In the second phase, the results of various 2D phase-sensitive correlated experiments (DQF-COSY, TOCSY) were combined to delineate scalar connectivities and identify spin system to specific side chains.

Leu35, Leu64, Leu68, Leu94, and Leu98. The cross-peaks connecting methine or methylene protons with a methyl group are usually a prominent feature in 2D NMR spectra of Im−cyt *c*. Leu and Val give rise to a pair of methyl cross-peaks at the same methine proton chemical shift, but an unambiguous distinction can be obtained on the basis of the multiplet pattern, which cross-peaks belong to the same residue. In the case of Leu98, in 2D EXSY spectrum (Figure 3), Leu98 δ_2H_3, δ_1H_3 of cyt *c* are known to resonate at 0.03 ppm and 0.46 ppm. From the cross-peaks (-0.40, 0.03) and (0.06, 0.46), we can assign Leu98 δ_2H_3, δ_1H_3 of Im−cyt *c* at −0.40 ppm and 0.06 ppm. The present data definitely identify the pairs of δH_3 protons in the upfield window of DQF-COSY and TOCSY spectra (Figure 4). TOCSY experiments provid relayed βH-δH_3, and αH-γH connectivities in Leu, which enables observation of the entire spin system. In this way, spin systems of Leu35, Leu64, Leu68, and Leu94 are assigned.

Ile9, Ile57, Ile75, Ile81, Ile85, and Ile95. Ile gives rise exclusively to the ^{1}H spin system $A_3MPT(B_3)X$; it contains a methyl group which is coupled to two other protons. This unique feature should in all case be sufficient for an unambiguous distinction of δH_3 from its γH_3 and the methyl groups of Val and Leu. Chemical shifts at −0.22, −0.02, 0.62, 0.91, 1.06, 0.49, and 1.91 ppm in 2D EXSY spectrum are assigned to Ile57 δH_3, Ile85 δH_3, γH_3, Ile81 δH_3, γH_3, Ile95 δH_3, and Ile75 δH_3 of cyt *c*[4], and their corresponding chemical shifts at 0.25, 0.23, 0.87, 0.37, 0.47, 0.81, and 1.80 ppm can be assigned to the same groups of Im−cyt *c* respectively (Figure 3), by which each Ile residues as well as Leu residues can be discriminated. Of the six isoleucines, most of residues exhibit long-rang *J*-connectivities from βH to δH_3, γH to αH, and γH to γH_3, so the side chains of them are assigned in TOCSY spectra (as

(19) Mclachlan, S. J.; La Mar, G. N.; Lee, K. B. *Biochim. Biophys. Acta* **1988**, *957*, 430.
(20) La Mar, G. N.; de Ropp, J. S.; Chacko, V. P.; Satterlee, J. D.; Erman, J. E. *Biochim. Biophys. Acta* **1982**, *708*, 317.

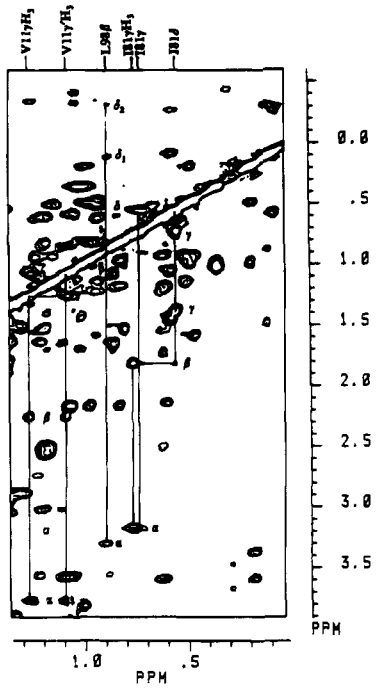

Figure 4. Section of phase sensitive TOCSY spectrum of [$^2H_4$]Im−cyt *c* ($C_{cyt\ c}$ = 8 mM, $C_{[^2H_4]Im}$ = 1.0 M) at 319 K and pH 7.0 obtained with a mixing time of 50 ms.

illustrated in Figure 4) in combination with DQF-COSY data. For Ile95, the search for long-range TOCSY connectivity failed at all mixing times and only γH and δH_3 are identified. The last unassigned Ile residue is Ile9. In 2D EXSY spectra, no exchange cross-peak is found for it. The reason may be that nearly no changes occur in the environment of this residue after Im binding to cyt *c* and, hence, cyt *c* and Im−cyt *c* have almost the same chemical shifts for Ile9. According to chemical shift of Ile9 δH_3 in native cyt *c*, the unassigned spin coupled system of Ile along with the long-range connectivity from γH to γH_3 in TOCSY is assigned to Ile9. The assignment of αH remains tentative owing to the missing related cross-peak from γH to αH.

Thr19, Thr28, and Thr78. The residue exhibits A_3MX spin system, which can easily be differentiated from other spin systems. Thr28 γH_3, Thr78 βH, and Thr19 βH of cyt *c* were known to resonate at 0.27, 5.70, and 5.40 ppm[4] respectively. From the EXSY cross-peaks in Figure 5, the protons of the same residues in Im−cyt *c* can be identified at 0.04, 6.27, and 5.48 ppm. By using DQF-COSY and TOCSY spectra, it is possible to trace the side chains completely.

Val3, Val11, and Val20. Val has a pattern containing two βH−γH_3 cross-peaks and one αH−βH cross-peak. For the three valines in Im−cyt *c*, DQF-COSY and TOCSY patterns identify their spin systems by αH−βH−γH_3, $\gamma' H_3$ cross-peaks as 3.75−2.24−1.08, 1.25 ppm, 3.54−2.15−1.05, 1.08 ppm and 4.52−2.14−0.84, 0.97 ppm (in Figure 4, Val11 is just one example). As compared with chemical shifts of Val protons of cyt *c*,[4] it is found that they are similar to Val11, Val3, and Val20 in turn, thus providing the assignments of Val3, Val11, and Val20 of Im−cyt *c*. The comparison of chemical shifts between Im−cyt *c* and cyt *c* also indicate the structure of N-terminal segment is largely unaffected by substitution of Met80 with imidazole.

3. Assignments of Side Chains of Aromatic Amino Acid Residues. Trp59. Resonance assignments of the single tryptophan residue in horse cytochrome *c*, Trp59, can be proposed for the indole ring protons. The DQF-COSY cross-peaks in Figure 6 exhibit the coupling pattern expected for the

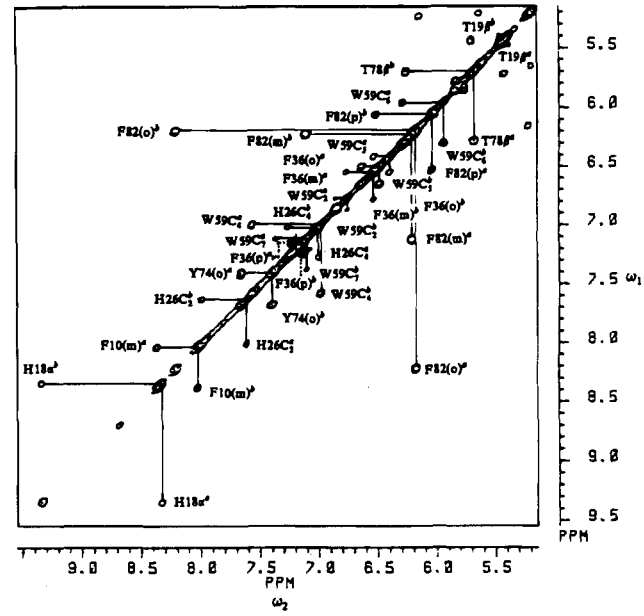

Figure 5. Aromatic region of the 2D EXSY spectrum of a sample containing comparable amounts of cyt *c* and [$^2H_4$]Im−cyt *c* ($C_{cyt\ c}$ = 8 mM, $C_{[^2H_4]Im}$ = 0.04 M) at 319 K and pH 7.0 with mixing time 50 ms. Chemical shifts of resonances for cyt *c* and [$^2H_4$]Im−cyt *c* are read in ω_2 dimension. *a* indicates cyt *c*; *b* indicates [$^2H_4$]Im−cyt *c*.

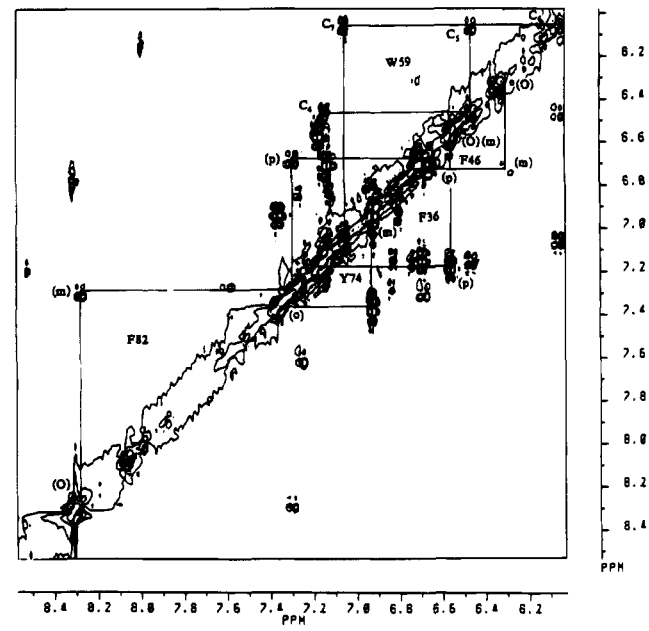

Figure 6. Aromatic region of phase sensitive DQF-COSY spectrum of [$^2H_4$]Im−cyt *c* ($C_{cyt\ c}$ = 8 mM, $C_{[^2H_4]Im}$ = 1.0 M) at 319 K and pH 7.0.

indole ring protons of Trp59 in Im−cyt *c*. Second nearest-neighbor coupling information is provided by a TOCSY experiment, which shows the apparent pattern does in fact link a linear network of protons. C_7H and C_4H resonances can be distinguished from peaks in 2D EXSY (Figure 5) on the basis of the assignment of Trp59 in cyt *c*.

Phe82, Phe36, Phe46, and Tyr74. The phenylalanine and tyrosine side-chain spin systems are most clearly defined in the DQF-COSY spectrum as demonstrated by the example of Phe82 shown in Figure 6. The rotationally averaged signals (C_2H merges with C_6H and C_3H with C_5H) at 6.20, 6.22, and 6.06 ppm in 2D EXSY spectrum originate from Phe82 (o), (m), and (p) protons of cyt *c*.[21] Their corresponding signals at 8.22, 7.12 and 6.52 ppm thus assign the identified spin system in DQF-

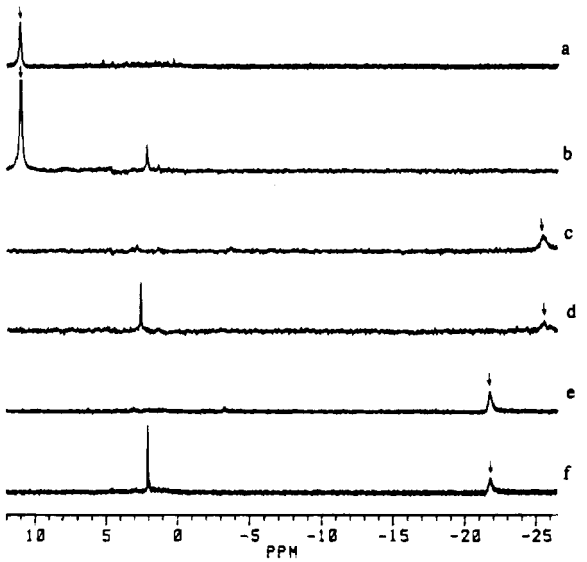

Figure 7. 1H NMR spectra at 319 K and pH 7.0. Parts b, d, and f show saturation transfer difference spectra of an equimolar mixture of cyt *c* and [$^2H_4$]Im−cyt *c* ($C_{cyt\ c}$ = 8 mM, $C_{[^2H_4]Im}$ = 0.04 M) with preirradiation of Met80 βH, γH, and ϵCH_3 of cyt *c*. Parts a, c, and e show NOE difference spectra with preirradiation of Met80 βH, γH, and ϵCH_3 of cyt *c*. The downward arrow indicates the peak being preirradiated.

COSY spectrum to the Phe82 (o), (m), and (p) protons of Im−cyt *c* respectively. So combining 2D EXSY and DQF-COSY spectra, we can assign the aromatic ring protons of Phe36 and Tyr74.

For the remaining two Phe residues, Phe10 and Phe46, one proton of the Phe10 ring of Im−cyt *c* can be defined through the 2D EXSY spectrum at 8.03 ppm (Figure 5), but the whole aromatic spin system remains unshown in our experiments, possibly because the Phe10 aromatic ring is undergoing relatively slow rotation and their resonances are broadened by chemical exchange. Therefore, the typical spin system of phenyl ring with the coupling pattern (o)−(m)−(p) at 6.35−6.74−6.66 ppm in the aromatic region of the DQF-COSY spectrum is assigned to Phe46 (Figure 6). Long-range connectivity from (p) to (o) in the TOCSY spectrum is shown to consistant with the assignments for Phe46.

4. Assignments of Side Chains of Some Other Amino Acid Residues. Met80. For the protons of Met80, their cross-peaks in 2D EXSY spectra are too weak to be observed, possibly because the relaxation time T_1s of Met 80 protons in native cyt *c* (axial ligand) and Im−cyt *c* (non-axial ligand) differ widely. Multiple mixing times are advised, which requires a great deal of instrument time. So we have identified these protons using 1D saturation transfer experiments.

In the difference spectra of the mixture of cyt *c* and Im−cyt *c* with saturation of previously assigned Met80 βH, γH, and ϵCH_3 resonances of cyt *c*, magnetization is transfered to the corresponding resonances of Im−cyt *c* at 2.17, 2.52, and 2.00 ppm respectively (Figure 7b,d,f). This interpretation is confirmed by NOE difference spectra of cyt *c* with preirradiation of Met80 βH, γH and ϵCH_3 resonances (Figure 7a,c,e). The present data show that these groups give rise to sharpened signals with random coil ^1H chemical shifts, which indicate that the coordination bond of Fe−S between heme and Met80 is broken[22] and groups of Met80 (i.e. ϵCH_3) have moved into a position where the paramagnetic contribution to the resonances from Fe^{3+} is minor. In addition, preirradiation of the frequency of Met80 βH of cyt *c* causes saturation transfer not only to the Met80 βH of Im−cyt *c* but also to 5-CH_3 of Im−cyt *c* (not shown in Figure 7b). This is due to the fact that Met80 βH of cyt *c* overlaps with 5-CH_3 of cyt *c* at 319 K. On the basis of the chemical shifts of the assigned βH, γH of Met80 in Im−cyt *c*, we can locate the spin system of Met80 in DQF-COSY and TOCSY spectra and identify other proton (i.e. β'H and γH) chemical shifts of the residue.

His18. The resonance at 9.35 ppm in the spectrum of Im−cyt *c* has been assigned to His18 αH, which is found to be coupled with the line at 7.43 ppm in TOCSY spectra, thus providing the assignment of the other βH of His18. The failure to observe this cross-peak in DQF-COSY spectrum indicates the DQF-COSY map is uninformative for all protons close to iron due to both the rapid relaxation and increased line width. A rotating-frame correlation experiment which gives only positive cross-peaks (i.e., TOCSY) may provid the needed additional scalar connectivities.

His26. The chemical shifts of His26 C_2 and C_4 protons of cyt *c* have been assigned. From 2D EXSY (Figure 6), the corresponding resonances of Im−cyt *c* can be identified at 7.99 and 7.29 ppm respectively, which is supported by the four-bond coupling cross-peak (7.29,7.99) in TOCSY spectra.

All the resonance assignments of Im−cyt *c* are listed in Table 2.

II. Analysis of Conformation Changes Based on NOEs. The NOE can provide valuable information about the spatial arrangement of the amino acid residues in proteins and can be conveniently observed in both 1D NOE difference spectra and cross sections from the NOESY spectrum. For an elucidation of the structural changes occurring in the substitution of Met80 in cyt *c* by imidazole, it is necessary to compare all NOEs with those obtained in cyt *c*.

1. NOEs between Heme Methyl Groups and Residues around the Bound Imidazole. Parts a−d of Figure 8 are NOE difference spectra of Im−cyt *c* generated by preirradiation of heme methyl groups 1, 5, 3, and 8-CH_3. NOEs observed from 8−CH_3 to Leu35 δ_1H_3, δ_2H_3 and Leu64 δ_2H_3; from 3-CH_3 to thioether-4 (Te-4); from 5-CH_3 to Thr28 γH_3 and from 1-CH_3 to Leu98 δ_1H_3, δ_2H_3 and Leu94 δ_1H_3, δ_2H_3 have the same pattern in native cyt *c* and show that distances of these groups relative to their corresponding heme methyl groups do not change in an obvious manner. The only different situation is found with preirradiation of 1-CH_3 as a new NOE at Ile85 δH_3 (d = 6.85 Å in cyt *c*) and a weak NOE at Leu68 δ_2H_3 (d = 2.40 Å in cyt *c*) are observed, while the original NOE at Leu64 δ_2H_3 (d = 4.53 Å in cyt *c*) is enhanced. These results suggest that in Im−cyt *c*, as compared to native cyt *c*, Ile85 δH_3 and Leu64 δ_2H_3 move close to 1-CH_3, while Leu68 δ_2H_3 moves away from 1-CH_3.

2. NOEs between Amino Acid Residues around the Bound Imidazole. The NOE difference spectrum of Im−cyt *c* upon presaturation of Leu68 δ_2H_3 is shown in Figure 8e. NOEs, between Leu68 δ_2H_3 and Leu64 δ_2H_3, Leu94 δ_2H_3, Leu98 δ_2H_3 and Ile85 γH, which parallel those observed for cyt *c*, indicate nearly no changes occur in the relative positions of these groups as a result of Im binding. However, preirradiation of Leu68 δ_2H_3 yields two new NOEs arising from Leu98 δ_1H_3 (in cyt *c*, d = 5.40 Å) and Ile85 δH_3 (in cyt *c*, d = 6.90 Å) suggesting the movement of Ile85 toward Leu68 δ_2H_3 and

(21) Boswell, A. P.; Eley, C. G. S.; Moore, G. R.; Robinson, M. N.; Williams, G.; Williams, R. J. P.; Neupert, W. J.; Hennig, B. *Eur. J. Biochem.* **1982**, *124*, 289.

(22) Wooten, J. B.; Cohen, J. S.; Vig, I.; Schejter, A. *Biochemistry* **1981**, *20*, 5394.

Table 2. Assignment of Chemical Shifts (ppm) Some Spin Systems of Im−cyt *c*[a]

leucine residue	αH	βH	γH	δ_1H_3	δ_2H_3
35	4.31	1.85	0.56	0.05	0.30
64	3.98	1.37	1.03	0.36	0.43
68	4.51	0.93	1.24	0.35	1.30
94	3.81	0.60, 1.42	0.98	0.48	0.70
98	3.30	0.84, 1.66	1.47	0.11	0.32
isoleucine residue	αH	βH	γH	γH_3	δH_3
9	*b*	1.45	1.05, 1.45	0.61	0.58
57	4.16	1.56	0.91, 1.12	0.43	0.47
75	4.10	3.23	1.94, 2.22	*b*	1.80
81	3.19	1.82	0.76, 1.34	0.76	0.54
85	3.52	1.72	1.01	1.08	0.34
95	*b*	*b*	1.11, 1.68	*b*	0.85
threonine residue		αH	βH		γH_3
19		6.13	5.53		2.30
28		3.57	3.33		0.12
78		3.27	6.33		3.00
valine residue		αH	βH		γH_3
3		3.54	2.15		1.05, 1.08
11		3.75	2.24		1.08, 1.25
20		4.92	2.16		0.83, 0.97
methionine residue	αH	βH	γH		ϵCH_3
80	*b*	2.17, 2.31	2.52		1.99
tryptophan residue	C_4	C_5	C_6		C_7
59	7.14	6.44	6.04		7.04
phenylalanine residue		(o)	(m)		(p)
36		6.54	6.54		7.16
46		6.35	6.74		6.66
82		8.27	7.30		6.68
tyrosine residue		(o)			(m)
74		7.38			6.93
histidine residue		C_2			C_4
26		7.98			7.29

[a] Chemical shifts are given with respect to dioxane at 3.743 ppm, determined in the sample of Im−cyt c at pH 7.0, 319 K. [b] Not Determined.

a small shift of Leu68 δ_2H_3 relative to Leu98 δ_1H_3. In cyt *c*, Leu68 δ_2H_3 is at a distance of 3.53 Å to Met80 ϵCH_3, in Im−cyt *c*, NOE between Leu68 δ_2H_3 and Met80 ϵCH_3 is still observed, which indicates that when it is displaced by Im, Met80 is still close to Leu68 δ_2H_3 in Im−cyt *c*.

As shown in the upfield region of the phase-sensitive NOESY spectrum of Im−cyt *c* (Figure 9), all expected intraresidue NOESY cross-peaks are readily detected: 1 (Leu64 δ_2H_3; Leu64 δ_1H_3), 2 (Leu35 δ_2H_3; Leu35 δ_1H_3), 3 (Leu98 δ_2H_3; Leu98 δ_1H_3), 4 (Leu94 δ_2H_3; Leu94 δ_1H_3), 8 (Ile81 δH_3; Ile81 βH), 9 (Ile81 δH_3; Ile81 γ′H), 10 (Ile81 δH_3; Ile81 γH), 11 (Leu35 γH; Leu35 βH), 12 (Leu35 γH; Leu35 δ_1H_3), 13 (Leu35 γH; Leu35 δ_2H_3), 15 (Leu94 βH; Leu94 β′H), 16 (Leu94 βH; Leu94 δ_1H_3), 18 (Leu94 βH; Leu94 δ_2H_3), 19 (Ile81 γH; Ile81 βH), 20 (Ile81 γH; Ile81 γ′H), 21 (Leu98 βH; Leu98 β′H), 22 (Leu98 βH; Leu98 γH), 23 (Leu98 βH; Leu98 δ_1H_3), 24 (Leu98 βH; Leu98 δ_2H_3), 25 (Leu68 βH; Leu68 γH), 26 (Leu68 βH; Leu68 δ_1H_3), 27 (Leu94 γH; Leu94 β′H); 28 (Leu94 γH; Leu94 δ_1H_3); 29 (Leu94 γH; Leu94 δ_2H_3); 31 (Ile85 γH; Ile85 βH), 32 (Ile85 γH; Ile85 δH_3), 33 (Leu64 γH; Leu64 δ_1H_3), 35 (Leu64 γH; Leu64 δ_2H_3), 38 (Leu68 γH; Leu68 δ_1H_3), 39 (Leu64 βH; Leu64 δ_1H_3), 41 (Leu64 βH; Leu64 δ_2H_3), 42 (Leu94 β′H; Leu94 δ_1H_3), 43 (Leu94 β′H; Leu94 δ_2H_3), 44 (Leu98 γH; Leu98 δ_1H_3), 45 (Leu98 γH; Leu98 δ_2H_3), 46 (Ile 85 δH_3; Ile 85 βH), 47 (Leu98 β′H; Leu98 δ_1H_3), 48 (Leu98 β′H; Leu98 δ_2H_3), 49 (Leu35 βH; Leu35 δ_1H_3), 50 (Leu35 βH; Leu35 δ_2H_3), which confirm the above assignments. Contact between Leu98 δ_2H_3 and Leu94 δ_1H_3, Leu98 δ_2H_3 and Leu94 γH, and Leu94 δ_1H_3 and Leu98 δ_1H_3 is also clearly shown: 6 (Leu98 δ_2H_3; Leu94 δ_1H_3), 30 (Leu98 δ_2H_3; Leu94 γH), 5 (Leu94 δ_1H_3; Leu98 δ_1H_3). This means the distances between them are shorter than 5 Å and no obvious spatial change occurs as compared with that in cyt *c* (d_6 = 3.46 Å, d_{30} = 2.80 Å, d_5 = 3.40 Å). More importantly, some new NOESY cross-peaks from Leu94 βH to Ile85 βH (14), from Leu64 γH to Leu68 δ_1H_3 (34), from Leu68 γH to Met80 ϵCH_3 (36), and from Met80 γH to Ile81 δH_3 (7) are observed, which indicate large movements have happened to these groups, namely, Ile85 βH moves toward Leu94 βH from the original distance of 5.65 Å to one less than 5 Å; Ile85 δH_3 still keeps close with Leu94 βH at a distance shorter than 5 Å as demonstrated by the NOE peak 17 (Leu94 βH; Ile85 δH_3) (in cyt *c*, d_{17} = 4.90 Å); the distances of Leu68 γH to Met80 ϵCH_3 and Ile81 δH_3 to Met80 γH have changed from 5.77 and 5.84 Å in cyt *c* to distances of approximately 5 Å or less. These results suggest that after Met80 ϵCH_3 was substituted by imidazole, Ile85 moves toward Leu94 relatively, Met80 ϵCH_3 moves away from iron to the position near Leu68 δ_2H_3 and Leu68 γH. Met80 γH is in contact with Ile81 δH_3, thereby leaving room for Im binding to iron. The NOE connectivities linking Leu64 γH and Leu68 δ_1H_3 (34) and Leu64 βH and Leu68 δ_1H_3 (40) indicate that

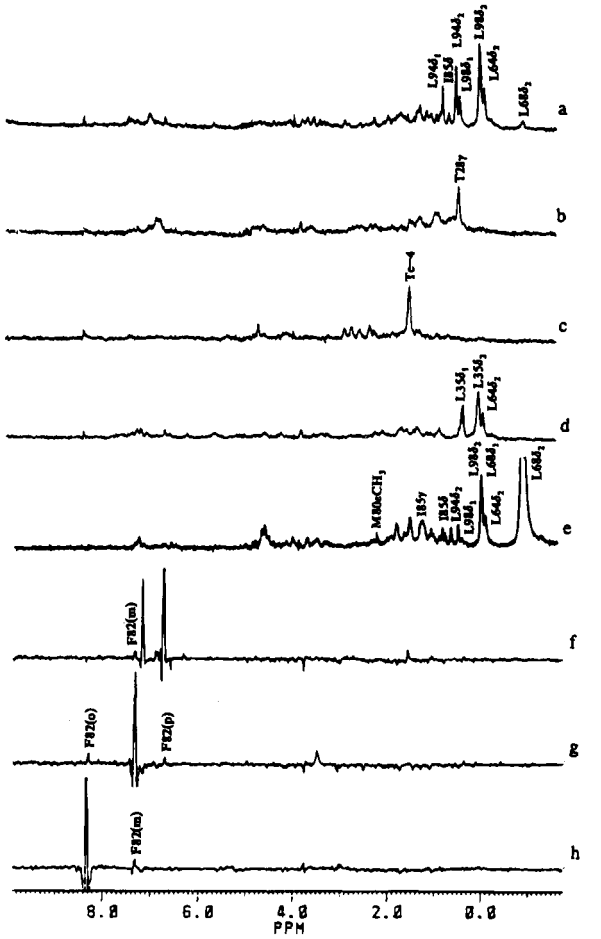

Figure 8. (a−e) NOE difference spectra of [$^2H_4$]Im−cyt *c* ($C_{cyt\ c}$ = 5 mM, $C_{[^2H_4]Im}$ = 1.0 M) at 319 K and pH 7.0 with saturation of heme methyl groups 1-CH_3, 5-CH_3, 3-CH_3, 8-CH_3, and Leu68 δ_2, respectively. (f−h) Rows extracted from the NOESY spectrum of [$^2H_4$]Im−cyt *c* ($C_{cyt\ c}$ = 8 mM, $C_{[^2H_4]Im}$ = 1.0 M) recorded with the mixing time of 150 ms at 319 K and pH 7.0 at Phe82 (p), Phe82 (m), and Phe (o) protons.

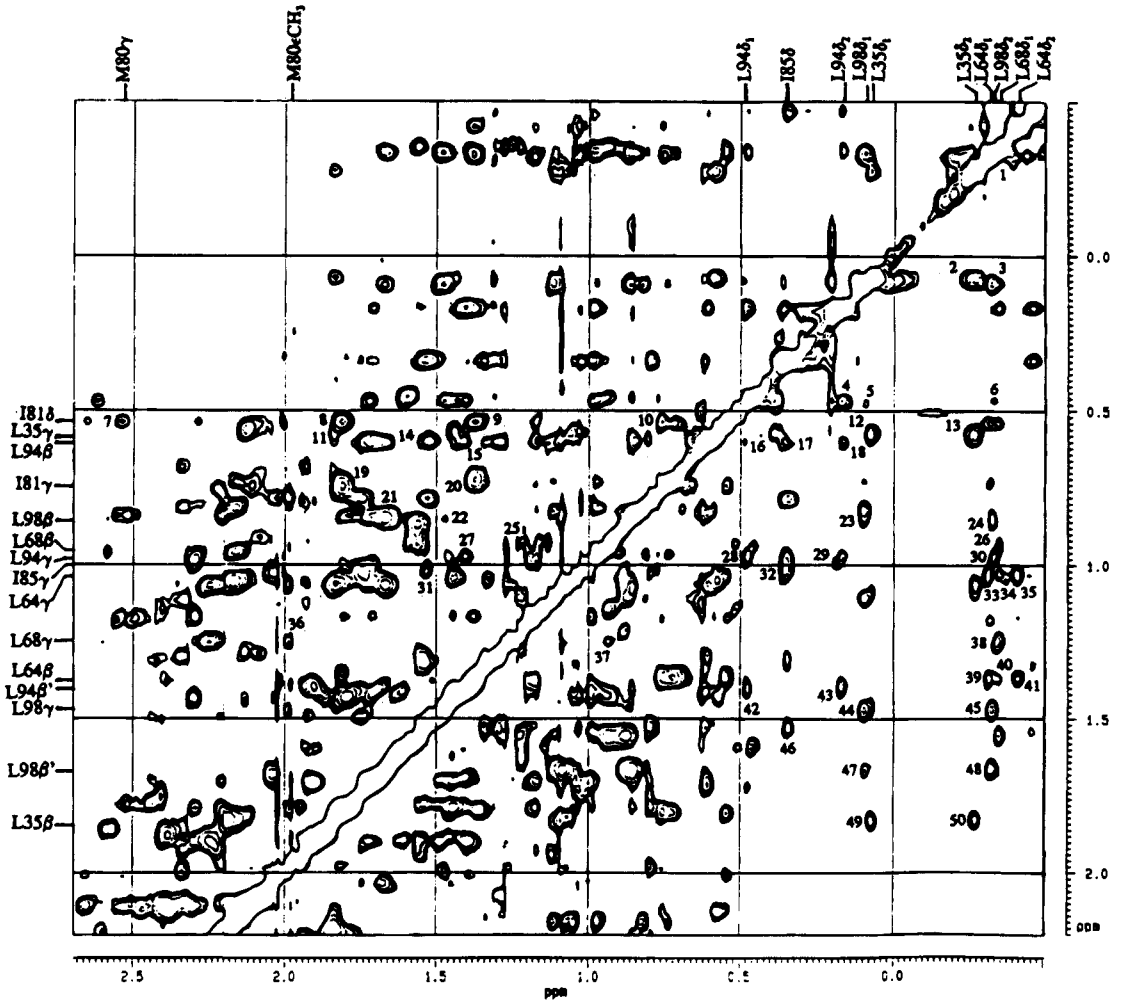

Figure 9. Region of the phase-sensitive NOESY spectrum of [$^2H_4$]Im−cyt *c* ($C_{cyt\ c}$ = 8 mM, $C_{[^2H_4]Im}$ = 1.0 M) with the mixing time of 150 ms at 319 K and pH 7.0. NOESY cross peaks are numbered 1−50 from the higher right and are described in the text.

Leu68 δ_1H_3 locates in a position close to both Leu64 γH and βH (in cyt *c*, d_{34}=5.78 Å, d_{40}=3.74 Å) in Im−cyt *c*.

Figure 8f−h shows the rows extracted from the NOESY spectrum of Im−cyt *c* at Phe82 (p), (m) and (o) protons. Contrary to observations for native cyt *c*, no NOEs are observed from these protons to their original neighboring residues and groups (i.e. thioether-2, thioether-4, 3-CH_3, Ile85, Met80 ϵCH_3, and Leu68 δH_3). In the aromatic region, no NOE is observed excluding its own phenyl protons, but in the aliphatic range, NOEs are observed only at 1.50 and 3.44 ppm (they possibly arise from its own βH and αH). These results suggest that the Phe82 side chain moves from a position of close-contact with the side chains of other residues due to the breakage of the Fe−S bond.

3. NOEs between the Bound Imidazole and the Residues around It. In order to elucidate the orientation and the environment of the bound Im, the NOE difference spectrum of Im−cyt *c* was obtained by presaturation of 2H of the bound Im (Figure 10). From NOEs at Leu64 δ_2H_3, Leu68 δ_2H_3, Leu98 δ_1H_3, Leu94 δ_1H_3, and Ile85 γH_3, δH_3, it can be concluded that these groups are located at a distance shorter than 5 Å near 2H of the bound Im. As compared with the environment of Met80 ϵCH_3 and γH in cyt *c* where Leu68 δH_3, Phe82 (p), (m) protons and Ile81 αH are at a distance of 5 Å or less relative to them, when presaturation of the resonance is performed at 2H of the bound Im, no NOE in Im−cyt *c* is observed at Phe82 (p), (m) and Ile81 αH, which indicate that they move away from the neighbor region of the axial ligand. These results

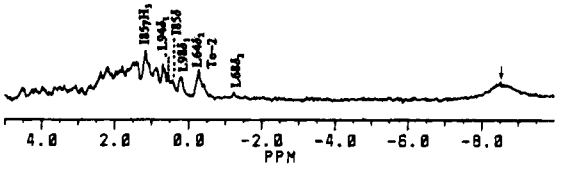

Figure 10. NOE difference spectrum of Im−cyt *c* ($C_{cyt\ c}$ = 5 mM, C_{Im} = 1.0 M) at 319 K and pH 7.0 with saturation of the 2H of the coordinated imidazole. The downward arrow indicates the peak being saturated.

suggest that after Met80 is displaced by Im, structural changes occur overwhelmingly on the methionine side of the heme in the environment of the axial ligand. The core accommodating exogenous ligand binding to iron has reorganized.

Additionally, NOE not only at Leu64 δ_2H_3, Leu68 δ_2H_3, Leu98 δ_1H_3, Leu94 δ_1H_3, and Ile85 δH_3 which are close to 1-CH_3 as shown in Figure 8a, but also at thioether-2 (Te-2) upon preirradiation of 2H of the bound Im (Figure 10) imply that the 2H of the bound Im is pointed toward pyrrole I, and the orientation of the bound Im plane is close to the N_1−N_3 vector of porphyrin. A convenient measure of the orientation of imidazole ligand was introduced by using the dihedral angle (ϕ) between the imidazole plane and a plane perpendicular to the porphyrin containing N_1 and N_3 atoms. Consideration of intramolecular nonbonded interaction between Im C_2 and C_4 hydrogens and the pyrrole nitrogens in bis(imidazole) complexes of model hemins suggests maximum steric repulsion at ϕ = 0° or 90° and minimum repulsion repulsion at ϕ = 45°.[23]

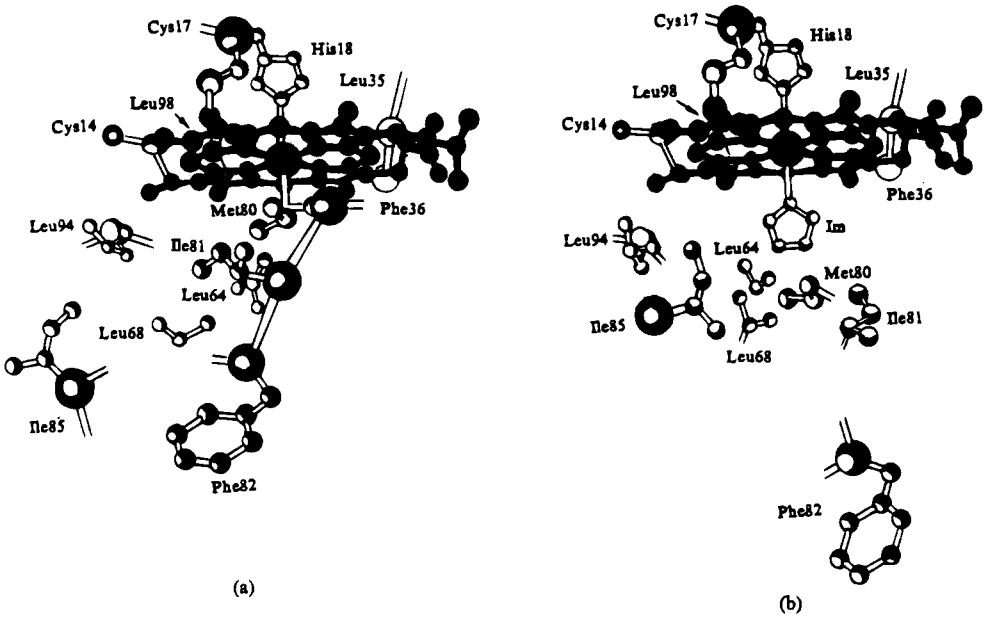

Figure 11. Schematic diagram of a proposed state in the conformational differences of heme pocket between cyt *c* and Im−cyt *c*: (a) native cyt c; (b) imidazole substituted cyt *c* (Im−cyt *c*). Pictures are modified from ref 30.

However, charge iterative extended Hückel theory calculations on electronic effect and numerous structures of model Fe(III) porphyrins coordinated to imidazole and most hemeproteins have long indicated that the interaction between imidazole and metal is orientationally ϕ dependent and favors small angles, namely the orientation very close to the N_1-N_3 porphyrin vector.[19,24-27] These clearly imply that ϕ-dependent bonding is the dominant factor.[24] The most extensive studies of the relationship between axial plane orientation and spectroscopic properties for the "class *b*" heme proteins indicate that a strong g_{max} EPR signals in which g_{max} is greater than 3, can be correlated with near-axial symmetry and in the case of planar axial ligands with perpendicular alignment of ligand planes such as in mitochondrial cyt b_{566} and b_{562} et al.[28] Concerning Im−cyt *c* complex, the heme protein exhibits EPR signals with characteristic *g* values of 2.96, 2.30, 1.58 similar to that of cytochrome b_5 and its model complex (TPP)Fe(Im)$_2$,[29] in which the planes of axial ligands are known to be nearly parallel.[27,28] The g_{max} EPR signal is thus indicative of parallel orientation of the two axial ligands under investigation. As the Im ring of His18 makes a 35° angle with a vector drawn through the N_1 and N_3 pyrrole nitrogen atoms in cyt *c*, if substitution of Met80 by Im has no influence on the orientation of His18, it is attractive to speculate that the two axial ligands make a small angle, or even parallel to each other, which does not give rise to a strong g_{max} EPR spectrum.[28]

The schematic digrame of a proposed state in the changes of structure of heme pocket of Im binding cytochrome *c* is shown in Figure 11. The full assignment and the determination of the overall protein fold of Im−cyt *c* are currently being carried out in our laboratory.

Conclusion

The hyperfine-shifted resonances and 25 spin systems of amino acid residues of Im−cyt *c* have been identified by analyses of 1D saturation transfer, 2D EXSY, DQF-COSY and TOCSY spectra. Some structural changes induced by Im displacing Met80 of cyt *c* in the heme pocket accommodating exogenous ligand binding to iron are offered. These changes include the following: Met80 ϵCH_3 moves to a position which is contact to both Leu68 γH and Leu68 δ_2H_3; Met80 γH is located in the region near Ile81 δH_3; Ile85 δH_3 shifts toward 1-CH_3 and Leu94 βH, and Ile85 βH is close to Leu94 βH; the Phe82 side chain makes a large movement relative to the original position due to the breakage of the Fe−S bond. These results suggest that the Fe−S bond is an important factor in preserving the conformation which is related to its biological function. NOE connectivities also indicate that 2H of the bound Im is close to not only thioether-2 but also groups of Leu64 δ_2H_3, Leu68 δ_2H_3, Leu98 δ_1H_3, Leu94 δ_1H_3, and Ile85 γH_3, δH_3, which are in contact with heme 1-CH_3; therefore, we speculate that the bound Im makes a small angle or even is parallel to the Im of His18 as supported by the EPR *g* values.

Acknowledgment. This research is fully supported by a grant from the National Natural Science Foundation China.

IC931467W

(23) Collins. D. M.; Countryman, R.; Hoard, J. L. *J. Am. Chem. Soc.* **1972**, *94*, 2066.
(24) Scheidt, W. R.; Chipman, D. M. *J. Am. Chem. Soc.* **1986**, *108*, 1163.
(25) Geiger, D. K.; Lee, Y. J.; Scheidt, W. R. *J. Am. Chem. Soc.* **1984**, *106*, 6336.
(26) Scheidt, W. R.; Geiger, D. K.; Haller, K. J. *J. Am. Chem. Soc.* **1982**, *104*, 495.
(27) Mathews, F. S.; Cdzerwinski, E. W.; Argos, P. In *The Porphyrins*; Dolphin, D., Ed.; Academic Press: New York, 1979; Vol. VII.
(28) Walker, F. A.; Huynh, B. H.; Scheidt, W. R.; Osvath, S. R. *J. Am. Chem. Soc.* **1986**, *108*, 5288.
(29) Walker, F. A.; Reis, D.; Balke, V. L. *J. Am. Chem. Soc.* **1984**, *106*, 6888.
(30) Ratilla, E. M. A.; Brother II, H. M.; Kostic, N. M. *J. Am. Chem. Soc.* **1987**, *109*, 4592.